Inorganic Chemistry

Article

pubs.acs.org/IC

X_2Y_2 Isomers: Tuning Structure and Relative Stability through Electronegativity Differences (X = H, Li, Na, F, Cl, Br, I; Y = O, S, Se, Te)

Majid El-Hamdi,[†] Jordi Poater,*[,†] F. Matthias Bickelhaupt,*[,‡,§] and Miquel Solà*[,†]

[†]Institut de Química Computacional and Departament de Química, Universitat de Girona, Campus de Montilivi, 17071 Girona, Catalonia, Spain

[‡]Department of Theoretical Chemistry and Amsterdam Center for Multiscale Modeling, VU University Amsterdam, De Boelelaan 1083, NL-1081 HV Amsterdam, The Netherlands

[§]Institute of Molecules and Materials, Radboud University Nijmegen, Heyendaalseweg 135, NL-6525 AJ Nijmegen, The Netherlands

Supporting Information

ABSTRACT: We have studied the XYYX and X_2YY isomers of the X_2Y_2 species (X = H, Li, Na, F, Cl, Br, I; Y = O, S, Se, Te) using density functional theory at the ZORA-BP86/QZ4P level. Our computations show that, over the entire range of our model systems, the XYYX isomers are more stable than the X_2YY forms except for X = F and Y = S and Te, for which the F_2SS and F_2TeTe isomers are slightly more stable. Our results also point out that the Y−Y bond length can be tuned quite generally through the X−Y electronegativity difference. The mechanism behind this electronic tuning is the population or depopulation of the π^* in the YY fragment.

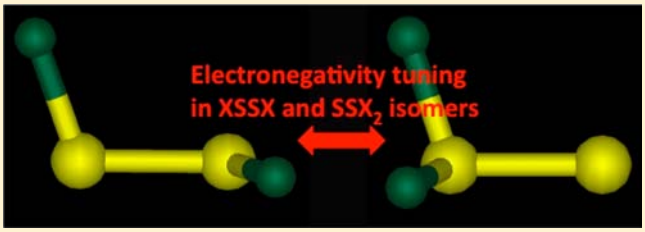

INTRODUCTION

The nature of the chalcogen−chalcogen bond in dichalcogenides and, particularly, in peroxides (XOOX) and disulfides (XSSX) has attracted considerable attention over the past decades.[1−4] Peroxides are highly reactive molecules that act as initiators of radical reactions[5] and as disinfectants and bleaches.[6] Their high reactivity is usually attributed to the weakness of the O−O bond.[7] These species also intervene in many oxygen-transfer reactions in industrial, biochemical, and atmospheric processes. Structural damage to a wide variety of biomolecules in some cases is the result of oxidation reactions by peroxide molecules.[8] On the other hand, disulfide compounds are important species in biochemistry and atmospheric reactions. In particular, the S−S bond formed by the oxidation of two cysteine residues in proteins plays a key role as the main stabilizer of the tertiary structures of proteins.[4] In addition, the disulfide/thiol system has been found to be relevant to control cell growth, proliferation, and human cancer development.[9]

From a theoretical point of view, calculations on X_2Y_2 dichalcogenides have been reported, among others, by Bickelhaupt and co-workers[10] (Y = S and X = F, Cl, H, and CH_3), Jursic[11] and Ornellas[12] (Y = S and X = F), Dobado et al.[13] (Y = O, S and X = H, F, CH_3), Kaur and collaborators[14] (Y = O, S, Se and X = H, CH_3, NH_2), Prascher and Wilson[15] (Y = S, Se and X = F, Cl, Br), and Zheng et al.[16] (Y = S and X = F, Cl, Br, I). These studies showed that the O−O and S−S bonds in XYYX compounds are special for two reasons. First, there is an important effect of the electronegativity of the substituent X on the Y−Y bond length, the O−O and S−S bonds being extremely short in FOOF[17−21] and FSSF.[10,11,22−26] In a valence bond approach, this has been attributed to the importance of ionic resonance structures of the $F^-−Y{=}Y^+−F$ type[17,18] in a so-called charge-shift bond.[27] In the molecular orbital theory, the partial depopulation of the π^*(np) of the Y_2 fragment in the formation of FYYF explains the short Y−Y bond length in these compounds.[10,18] Second, dihedral angles are, although this is sterically less favorable, close to 90° because, in this way, optimal electron-pair bonds between the $X^\bullet$ groups and the two π^* SOMOs of the $YY^{\bullet\bullet}$ fragment can be formed.[10] Interestingly, the potential energy surface for the rotation from the gauche to the trans conformation of XYYX is extremely flat.[28]

Although all X_2Y_2 systems exist in the XYYX form (C_2 symmetry; see Scheme 1), an isomeric hypervalent structure

Scheme 1

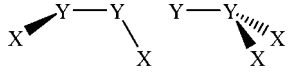

XYYX (C_2) **X_2YY** (C_s)

X_2YY (C_S symmetry) is also conceivable. These two isomers have been isolated and characterized for the case of disulfur difluoride species (difluorodisulfane FSSF and thiothionyl-fluoride F_2SS).[22−24,26,29−31] At temperatures above −100 °C, it was found that the FSSF isomer slowly isomerizes to F_2SS, and therefore, F_2SS is thermally more stable than FSSF.[31] However,

Received: October 28, 2012
Published: February 19, 2013

   dx.doi.org/10.1021/ic3023503 | Inorg. Chem. 2013, 52, 2458−2465

FSSF seems to be the most stable isomer at low temperatures as F_2SS is transformed into a molecular complex [FSSF,F_2SS] after cooling the sample down to −80 °C.[29] On the other hand, the heat of transformation of FSSF to F_2SS was determined experimentally[32] to be -11.3 ± 1.7 kJ mol^{-1} and the activation energy for this interconversion was found to be only 23.8 kJ mol^{-1}.[33] Although conflicting to some extent, these experimental results point out that the two disulfur difluoride isomers have similar energies. Theoretical calculations ruled out the possible direct unimolecular interconversion of FSSF to F_2SS in the ground state since calculated energy barriers are about 167.4 kJ mol^{-1}.[10,11] The possibility that the FSSF/F_2SS isomerization occurs via a bimolecular channel, which was based on the experimental evidence of the existence of the [FSSF,F_2SS] complex,[29] was also explored and found to be unlikely.[34] This suggests a more complex reaction mechanism that involves several elementary steps and, possibly, promotion to excited states of FSSF and F_2SS. In experiments, Cl_2S_2 has been found only in the form of ClSSCl.[35−37] Interestingly, however, mixing ClSSCl with F_2SS yields FSSCl.[16] Calculations indicate that the conversion of X_2SS toward XSSX becomes more exothermic[10] and goes with a lower barrier[16] when substituents X become less electronegative. Interestingly, FSeSeF was unambiguously identified by IR spectra. UV photolysis turned FSeSeF partially into $SeSeF_2$.[38] Finally, Cl_2Se_2 and Br_2Se_2,[35,39] which are used as plasma etchants in microelectronic devices,[40] are only found in the XSSX isomeric form.

From these previous results, it is clear that the electronegativity of X has a large impact on the molecular structure of XYYX species (in particular, the Y−Y bond length) and its relative stability as compared to the X_2YY isomer. In the present study, we have undertaken a detailed investigation of XYYX and X_2YY compounds for Y = O, S, Se, and Te (with special emphasis to the Y = S case) and X = H, Li, Na, F, Cl, Br, and I using the generalized gradient approximation (GGA) of density functional theory (DFT) at the BP86/QZ4P level. We aim at three objectives. First, we wish to obtain a set of consistent structural and thermochemical data for simple dicalchogenides (geometries, relative stabilities) all obtained at the same level of theory. This complements the available experimental and theoretical data, which are missing for some XYYX and most of the X_2YY species, and it enables a systematic analysis of trends. Second, our main purpose is to better understand the physics and the nature of the X−Y bond based on quantitative molecular orbital (MO) theory as contained in Kohn−Sham DFT.[41] Through a quantitative bond energy decomposition, we assess the importance of electrostatic attraction and orbital interactions for providing the X−Y bond, and we reveal the effect of the electronegativity of X in determining trends therein along the series X = H, Li, Na, F, Cl, Br, and I. The third objective is to further generalize the valuable tuning principle according to which the central Y−Y link in XYYX can be tuned from single bond to double bond by varying the electronegativity difference across the X−Y bond.

THEORETICAL METHODS

Many theoretical methods fail to correctly reproduce the molecular structure of XYYX and especially that of dioxygen difluoride, giving too short or too long bond distances.[20] In general, however, it is found that DFT performs reasonably well for predicting the equilibrium geometry of these species.[10,20,21] We used the BP86 functional[42−44] with the nonlocal corrections for exchange (Becke88) and correlation (Perdew86) included self-consistently. All DFT calculations were performed with the Amsterdam Density Functional (ADF) program.[45,46] The MOs were expanded in a large uncontracted set of Slater-type orbitals (STOs) of quadruple-ζ quality containing diffuse functions for all atoms and augmented with four sets of polarization functions (two *d* and two *f* functions for Li, O, F, Na, S, Cl, Se, Br, Te, and I, and two *p* and two *d* for H), the so-called QZ4P basis set. Polarization functions are essential to correctly describe the hypervalent X_2YY species.[47−49] To reduce the computational time needed to carry out the calculations, the frozen core approximation has been used. In this approximation, the core density is obtained and included explicitly, albeit with core orbitals that are kept frozen during the SCF procedure. Thus, in this work core electrons (1s for second period, 1s2s2p for third−fourth period, 1s2s2p3s3p4s3d for fifth period) were kept frozen during the geometry optimizations.[46] An auxiliary set of *s*, *p*, *d*, *f* and *g* STOs was used to fit the molecular density and to represent the Coulomb and exchange potentials accurately in each self-consistent field cycle.[50] Both relativistic effects through ZORA approximation,[51] and dispersion corrections through the Grimme-D_3 procedure[52] were considered for the Te_2X_2 species (those, in principle, more affected by relativistic and dispersion corrections), but we observed that they have a minimal effect (see Table S5 in the Supporting Information), and therefore, they were not applied.

An energy decomposition analysis (EDA)[41,53−57] has been carried out considering the process $YY^{\bullet\bullet} + 2X^{\bullet} \rightarrow X_2YY/XYYX$ that implies three fragments and corresponds to the interaction of Y_2 diradical fragment with the two X radicals. In the EDA analysis, the total bonding energy ΔE is made up of two major components: $\Delta E = \Delta E_{prep} + \Delta E_{int}$. In this formula, the preparation energy ΔE_{prep} is the amount of energy required to deform the fragments considered from their equilibrium structure to the geometry that they acquire in the overall molecule. The interaction energy ΔE_{int} corresponds to the actual energy change when these geometrically deformed fragments are combined to form the final molecule. It is analyzed in the framework of the Kohn−Sham MO model using a quantitative decomposition of the bond into electrostatic interaction, Pauli repulsion (or exchange repulsion or overlap repulsion), and (attractive) orbital interactions: $\Delta E_{int} = \Delta V_{elstat} + \Delta E_{Pauli} + \Delta E_{oi}$. The term ΔV_{elstat} corresponds to the classical electrostatic interaction. The Pauli repulsion term, ΔE_{Pauli}, comprises the destabilizing interactions between occupied orbitals and is responsible for the steric repulsion. This repulsion is caused by the fact that two electrons with the same spin cannot occupy the same region in space. The orbital interaction ΔE_{oi} in any MO model, and therefore also in Kohn−Sham theory, accounts for electron-pair bonding, charge transfer (i.e., donor−acceptor interactions between occupied orbitals on one moiety with unoccupied orbitals of the other, including the HOMO−LUMO interactions), and polarization (empty−occupied orbital mixing on one fragment due to the presence of another fragment). Since the Kohn−Sham MO method of density functional theory (DFT), in principle, yields exact energies and, in practice, with the available density functionals for exchange and correlation, rather accurate energies, we have the special situation that a seemingly one-particle model (an MO method), in principle, completely accounts for the bonding energy. Finally, in the bond-energy decomposition, open-shell fragments were treated with the spin-unrestricted formalism, but for technical reasons, spin-polarization was not included. This error causes the studied bond to become in the order of a few kJ mol^{-1} too strong. To facilitate a straightforward comparison, the EDA results were scaled to match exactly the regular bond energies. This scaling by a factor of ca. 0.98 in all model systems does not affect trends.

RESULTS AND DISCUSSION

In this section, first, the results for the XSSX and X_2SS isomers concerning their structure and stability will be presented (X = H, Li, Na, F, Cl, Br, and I). In the second part, the equivalent results for the XYYX and X_2YY (Y = O, Se, and Te) isomers will be discussed.

dx.doi.org/10.1021/ic3023503 | Inorg. Chem. 2013, 52, 2458−2465

Table 1. Geometrical Parameters of XSSX, X_2SS, XOOX, and X_2OO Isomers (Bond Lengths in Å and Angles in deg), Voronoi Charges of X and Y Atoms (in Electrons), and Isomerization Relative Energies (in kJ mol^{-1})[a]

X	r_{Y-Y}	r_{X-Y}	∠YYX	∠XYYX	Q(X)	$Q(Y_1)$	$Q(Y_2)$	r_{Y-Y}	r_{X-Y}	∠YYX	∠XYYX	Q(X)	ΔE_{rel}[b]
				X_2SS							XSSX		
F	1.875	1.655	108.2	98.8	−0.111	−0.116	0.339	1.896	1.676	110.2	88.1	−0.132	1.3
Cl	1.891	2.166	110.2	107.2	−0.120	−0.066	0.306	1.938	2.115	111.0	87.7	−0.109	−41.0
Br	1.896	2.355	110.8	109.5	−0.108	−0.053	0.268	1.940	2.289	111.6	87.6	−0.090	−43.1
I	1.908	2.597	111.9	112.4	−0.076	−0.058	0.210	1.961	2.497	111.8	86.6	−0.048	−50.2
H	1.977	1.383	108.9	94.6	0.082	−0.336	0.171	2.071	1.358	98.7	90.8	0.038	−100.4
Li	2.204	2.225	60.3	117.9	0.322	−0.322	−0.322	2.204	2.225	60.3	117.9	0.322	
Na	2.230	2.572	64.3	135.7	0.475	−0.475	−0.475	2.230	2.572	64.3	135.7	0.475	
				X_2OO							XOOX		
F	1.175	1.683	110.4	108.9	−0.194	0.088	0.299	1.200	1.608	111.2	89.3	−0.170	−50.2
Cl	1.208	2.100	114.6	117.0	−0.116	0.035	0.197	1.282	1.881	113.9	85.3	−0.053	−73.6
Br	1.219	2.245	115.9	119.0	−0.086	0.012	0.160	1.283	2.034	115.0	84.2	−0.031	−72.0
I	1.235	2.446	118.5	119.3	−0.048	−0.023	0.118	1.334	2.149	115.2	79.9	0.019	−79.5
H	1.536	0.978	100.6	109.2	0.237	−0.445	−0.029	1.469	0.975	99.9	112.8	0.153	−196.2
Li	1.585	1.734	62.8	179.7	0.393	−0.393	−0.393	1.585	1.734	62.8	179.7	0.393	
Na	1.601	2.092	67.5	179.9	0.507	−0.507	−0.507	1.601	2.092	67.5	179.0	0.507	

[a]Calculated r_{S-S} for S_2 is 1.912 Å and r_{O-O} for O_2 is 1.221 Å. [b]CCSD(T)/cc-pVQZ relative energies for Y = S are 7.4, −54.2, −57.5, and −117.1 kJ mol^{-1} for X = F, Cl, Br, and H, respectively.

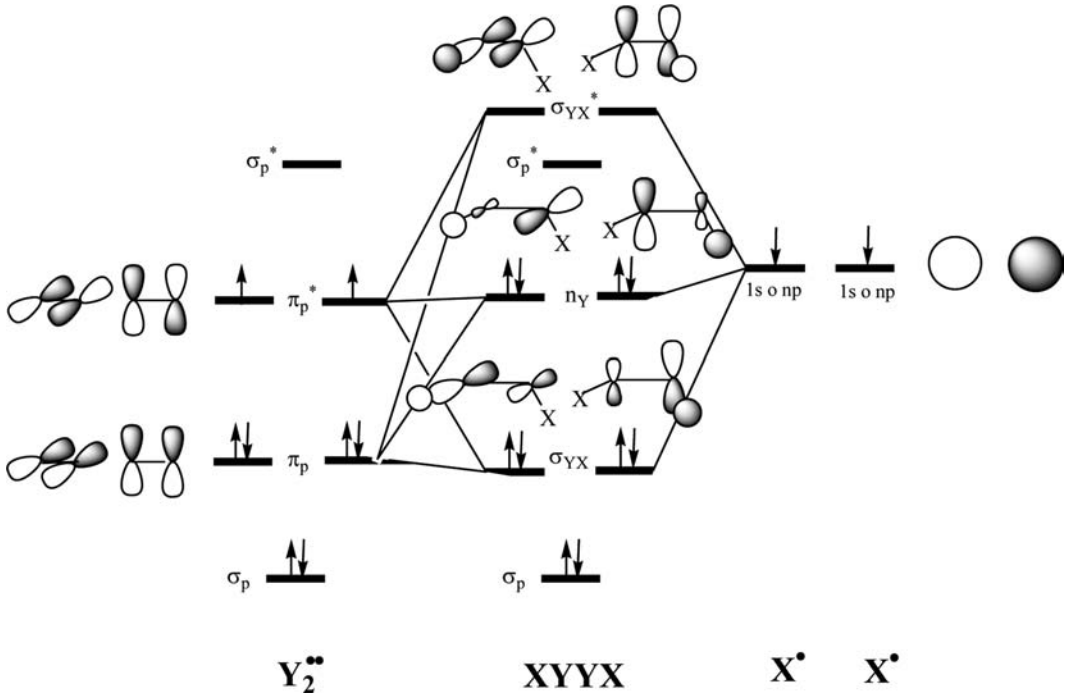

Figure 1. Molecular orbital diagram for the interaction of $Y_2^{••}$ with two $X^•$ to yield isomer XYYX.

XSSX and X_2SS Isomers. The most relevant geometrical parameters referred to the equilibrium structures of both XSSX and X_2SS are contained in Table 1. For X = H, F, Cl, Br, and I, we get the two expected symmetry conformations: C_2 for XSSX and C_s for X_2SS. On the other hand, for X = Li and Na, we have a unique isomer, with a rhombic tetrahedron shape. The S−S bond length gets longer with the decrease of the electronegativity of X along the series F < Cl < Br < I < H < Li < Na, being longer in XSSX than in X_2SS (Figure S1 in the Supporting Information shows the good correlation existent between Pauling electronegativity of X and the S−S bond length). Molecular S_2 in its triplet ground state presents a S−S bond length of 1.912 Å at the BP86/QZ4P level of theory, longer than the S−S bond in FSSF (1.896 Å) and in X_2SS (in the range of 1.875−1.908 Å for X = F, Cl, Br, and I), thus indicating that, in these compounds, the S−S bond has a higher double bond character than in the S_2 molecule. For the series X = H, F, Cl, Br, and I, the X−S bond length increases with the size of X, but in this case, X_2SS presents longer X−S, except for X = F. The ∠SSX angle opens up slightly for larger X in both XSSX and X_2SS species. The ∠XSSX dihedral angle in the XSSX isomer is close to 90° in all cases.

Table S2 in the Supporting Information contains the experimental data available for some of the compounds under analysis, as well as some higher-level calculations. In all cases, the calculated BP86/QZ4P parameters are close to the experimental ones, with differences for the X−S and S−S bond lengths of only a few hundredths of an Ångström or a few

dx.doi.org/10.1021/ic3023503 | Inorg. Chem. 2013, 52, 2458−2465

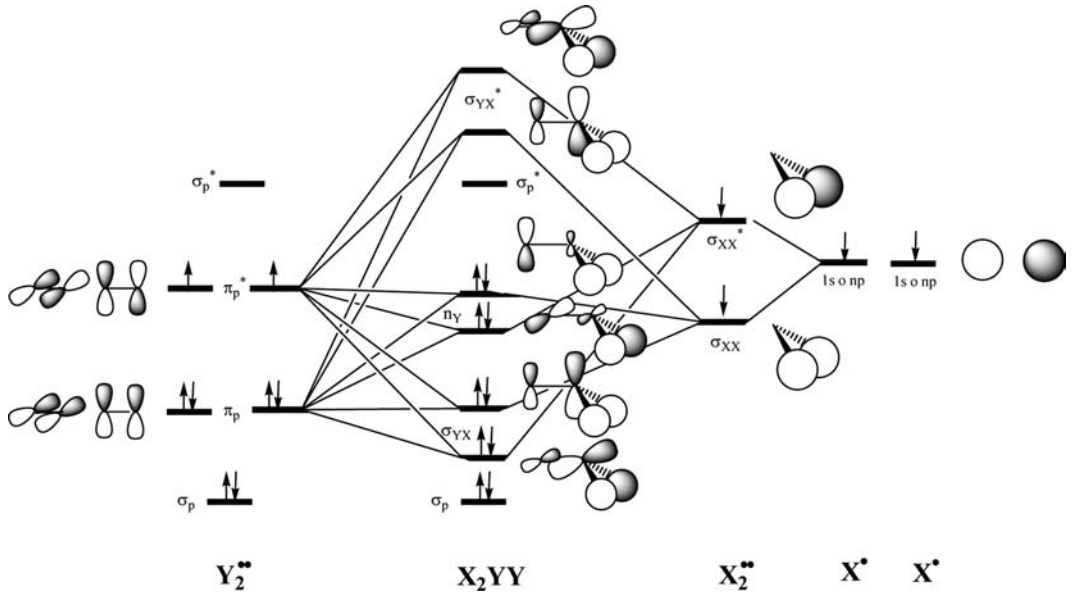

Figure 2. Molecular orbital diagram for the interaction of $Y_2^{\bullet\bullet}$ with two $X^{\bullet}$ to yield isomer X_2YY.

Table 2. Energy Decomposition Analysis for XSSX and X_2SS Isomers (in kJ mol^{-1}), Together with the Average Population of the Two SOMO Orbitals of SS (in Electrons), and Energy of the SOMO Orbital for X (in eV)

isomer	ΔE_{Pauli}	ΔV_{elstat}	ΔE_{oi}	ΔE_{int}	ΔE_{prep}	ΔE	P (π^*(SS))	E (X_{SOMO})
FSSF	2388.9	−978.9	−2132.3	−722.3	0.4	−721.9	0.71	−11.217
F_2SS	2594.2	−1059.0	−2260.4	−725.2	1.9	−723.2	0.69	−11.217
ClSSCl	1700.5	−765.0	−1383.5	−447.9	0.9	−447.0	0.96	−8.701
Cl_2SS	1467.0	−666.8	−1207.0	−406.8	0.6	−406.1	0.88	−8.701
BrSSBr	1409.3	−669.6	−1110.5	−370.8	1.1	−369.7	1.00	−7.996
Br_2SS	1166.8	−560.2	−933.5	−326.9	0.3	−326.6	0.91	−7.996
ISSI	1243.9	−610.5	−936.4	−303.0	3.1	−299.9	1.14	−7.248
I_2SS	943.3	−467.5	−725.5	−249.7	0.0	−249.7	1.00	−7.248
HSSH	1366.7	−631.0	−1331.9	−596.3	26.8	−569.5	1.39	−6.626
H_2SS	1263.1	−603.2	−1134.2	−474.2	5.3	−468.9	1.27	−6.626
LiSSLi/Li_2SS	1011.2	−650.1	−958.1	−597.0	74.6	−522.5	1.82	−2.955
NaSSNa/Na_2SS	694.1	−458.6	−675.7	−440.3	85.1	−355.1	1.88	−2.841

degrees for angles. In addition, Table S8 (Supporting Information) contains the comparison of the calculated relative isomerization energies with those at the CCSD(T) level of theory. It is observed that, in general, there is a good correspondence between the two methodologies with the trends being the same, thus proving the good behavior of the BP86/QZ4P level of theory.

With respect to the relative energies given in Table 1, in all cases except for X = F, the isomer XSSX is more stable than X_2SS, and the energy difference increases with the electronegativity of X from Cl (−41.0 kJ mol^{-1}) to H (−100.4 kJ mol^{-1}). For X = F, both isomers are almost isoenergetic, F_2SS being only 1.3 kJ mol^{-1} more stable than FSSF. This result is not far from the experimentally obtained −11.3 ± 1.7 kJ mol^{-1} corresponding to the FSSF-to-F_2SS transformation[32] and close to previous theoretical estimations (−21.3 kJ mol^{-1} at MP2/6-311++G(2df)[16] and −6.7 kJ mol^{-1} at QCISD(T)/6-31G(df)//MP2/6-31G(d,p)[10]). Most theoretical methods find FSSF and F_2SS close in energy, although some of them give F_2SS more stable than FSSF, whereas others yield the opposite.[10,11]

Now we proceed to analyze the corresponding MOs to get a better comprehension of the corresponding stabilities and structures of both isomers. Figure 1 depicts the MO diagram for the XYYX system. The diagram of Y_2 is that corresponding to a standard diatomic molecule, with σ_p and σ_p* orbitals formed by np_z atomic orbitals of Y = S (but the same is found for Y = O, Se, and Te), and π_p and π_p* formed by np_x and np_y ones. The $Y_2^{\bullet\bullet}$ fragment has a triplet state with two unpaired electrons in π_p* single occupied molecular orbitals (SOMO). The SOMOs of $X^{\bullet}$ interact with the π_p* and π_p orbitals of $Y_2^{\bullet\bullet}$ and lead to the formation of six orbitals that are doubly degenerated (two bonding σ_{YX}, two antibonding σ_{YX}*, and two nonbonding n_Y) and occupied with eight electrons. This comes down to forming two X−Y electron-pair bonds involving the two perpendicular π_p* SOMOs of YY, which explains the dihedral ∠XSSX close to 90°. It is obvious that, when $X^{\bullet}$ becomes less electronegative, π_p* orbitals have a more important role in the bonding, explaining the lengthening of the S−S distance with the decrease of electronegativity. This agrees with IR frequency studies showing that the frequency for the S−S bond decreases in the order FSSF > ClSSCl > BrSSBr.[29,58] The relatively long X−S bonds can be ascribed to the destabilizing interactions of the X groups with the closed-shell S−S bonding π_p orbitals.

On the other hand, for the X_2YY isomer, Figure 2 depicts the corresponding MO diagram. Starting from infinitely separated

dx.doi.org/10.1021/ic3023503 | Inorg. Chem. 2013, 52, 2458−2465

$X^{\bullet}$ fragments, one can approach the two $X^{\bullet}$ fragments and generate the positive (σ_{XX}) and negative (σ_{XX}^*) combination of the SOMOs of $X^{\bullet}$ that interact with the π_p^* and π_p orbitals of $Y_2^{\bullet\bullet}$ and drive to the formation of six nondegenerate orbitals (two bonding σ_{YX}, two antibonding σ_{YX}^*, and two nonbonding n_Y) with eight electrons. The contribution of the π_p^* orbitals in the occupied orbitals is somewhat smaller in this X_2SS isomer if one takes into account that, for all X, the S−S bond is shorter than that in the XSSX species. The effect of the electronegativity of $X^{\bullet}$ on S−S bonds is the same as that for the XSSX isomer. The X−S bond in X_2SS is longer than that in XSSX (except for X = F), which can be ascribed to a stronger steric repulsion between $X^{\bullet}$ groups when they bind to the same sulfur atom. Therefore, from the MO diagrams above, we can justify the longer S−S bond lengths in XSSX than in X_2SS because of the larger participation of the antibonding π_p^* orbitals in the former, especially for the heavier X substituents. It is likely that the fact that π_p^* orbitals participate more in XSSX than in X_2SS is because X−S can become stronger in XSSX as there is less steric X···X repulsion.

For X = Li and Na, we get the opposite case to X = F. Now 2s and 3s orbitals for Li and Na, respectively, are really high in energy; thus the corresponding electrons go to the π_p^* orbital of S−S, which causes the long S−S bond lengths and a system that can be simplified as an ionic $X^+S_2^{2-}X^+$. This shows up in the π^* populations (averaged over π_{px}^* and π_{py}^*) of the XSSX species which go from 1 in $SS^{\bullet\bullet}$ to 0.71 (X = F), 0.96 (X = Cl), 1.00 (X = Br), 1.14 (X = I), 1.39 (X = H), 1.82 (X = Li), and 1.88 (X = Na; see Table 2). This trend in π^* populations is also confirmed by the VDD atomic charges of Table 1. Thus, we find a net electron flow from the $S_2^{\bullet\bullet}$ fragment to $X^{\bullet}$ for X = halogen (−0.132, −0.109, −0.090, and −0.048 e are the Voronoi charges on the halogen atom in FSSF, ClSSCl, BrSSBr, and ISSI, respectively), whereas the opposite is found for X = H, Li, and Na (0.038, 0.322, and 0.457 e on H, Li, and Na atoms of HSSH, LiSSLi, and NaSSNa, respectively). The charge on $X^{\bullet}$ (X = halogen) is more negative for X_2SS than XSSX with the exception of X = F. The geometry of these $X^+S_2^{2-}X^+$ (X = Li and Na) does not correspond to the usual C_2 or C_s isomers, but to a rhombic tetrahedral structure. In this structure, the S−S bond length is close to that of a single S−S bond. The reason for the change in the molecular structure is related to the increased contribution of π(SS) donating back into X(ns) orbitals. In XSSX (X = Li and Na), the originally neutral SS fragment starts becoming effectively negatively charged, and that, in turn, makes the π MOs better donor orbitals. These π orbitals favor a bridging structure as soon as X becomes rather large and diffuse, that is, for X = Li and Na, but not in H.

With the aim of a better comprehension of the nature of the X−S bond in both isomers, an energy decomposition analysis has been carried out (see Table 2). As mentioned above, we have considered the process $SS^{\bullet\bullet} + 2X^{\bullet} \rightarrow X_2S_2/XSSX$. Results in Table 2 show that the ΔE_{prep} term is, in all cases, very small except for X = Li and Na. In these latter cases, the S−S bond length in the disulfide is large for the reasons explained above and ΔE_{prep} is about 80 kJ mol^{-1}. With the exception of X = F, the interaction energy and the bonding energy are more stabilizing for the isomers XSSX than X_2SS, and the difference increases when the electronegativity of X decreases. Along X = F to I, the X−S bond becomes less polar and thus less stable for both X_2SS and XSSX (see Table 2).[59−61] However, in the former, the X−S bond weakens more quickly because it is also more and more hampered by the increasingly bulky X. Thus, while for X = F, the isomers are within some 4 kJ mol^{-1} of equal energy, the gap between X_2SS above XSSX increases as X becomes more electronegative. A seemingly irregular behavior is observed for X = H, in which case H_2SS is significantly higher in energy than HSSH. In this case, we deal with the consequence of the very short hydrogen−element (here: H−S) bond distance, which, in turn, translates in a short, destabilizing H−H contact in the H_2SS isomer. Because of the shorter X−S bond length, isomers XSSX present larger values (in absolute value) of ΔV_{elstat}, ΔE_{Pauli}, and ΔE_{oi} than X_2SS, with the exception of X = F. Longer X−S distances cause smaller Pauli repulsion, as well as smaller electrostatic and orbital interactions (in absolute value). If we now compare the attractive terms ΔV_{elstat} and ΔE_{oi} for XSSX and X_2SS isomers, we see that $\Delta\Delta V_{elstat}$ and $\Delta\Delta E_{oi}$ differences between XSSX and X_2SS isomers favor the XSSX, except for X = F. In this latter case, the enhanced charge transfer and polarization promoted by the higher electronegativity of F (see Voronoi charges in Table 1) increases the contribution of double ionic resonance structure **b** (Figure 3) that is more stabilizing in F_2SS than

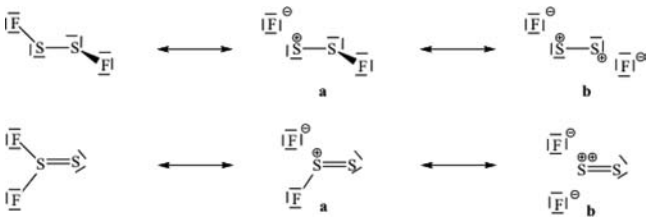

Figure 3. Some resonance structures for FSSF and F_2SS isomers.

FSSF. As a consequence, the two isomers become almost isoenergetic. This effect is more pronounced when the difference of electronegativity between X and Y is larger, and this is the case for F_2S_2. Moreover, it provides a rationale for the F−S distance in F_2SS that is shorter than that in FSSF.

XYYX and X_2YY Isomers (Y = O, Se, and Te). The most relevant geometrical parameters referred to the equilibrium structures of both XOOX and X_2OO are listed in Table 1. Table S3 in the Supporting Information compares the calculated BP86/QZ4P parameters with experimental data and calculations available for some of the compounds analyzed. It is found that, in most of the cases, BP86/QZ4P parameters are quite close to those obtained experimentally, the main exception being the ClOOCl species, for which calculated bond lengths present non-negligible differences from experimental values. The O−O bond length gets longer with the decrease of the electronegativity of X along the series F < Cl < Br < I < H < Li < Na. As for the X_2S_2 isomers, this O−O bond distance is longer in XOOX than in X_2OO with the exception of X = H. Molecular O_2 in its triplet ground state presents a O−O bond length of 1.221 Å at the BP86/QZ4P level of theory, longer than the O−O bond in FOOF and in X_2OO (X = F, Cl, and Br). However, at variance with I_2SS, I_2OO has a longer O−O bond than O_2, thus indicating that, in this compound, the O−O bond has a slightly lower double bond character than in the O_2 molecule. This change can be explained by the higher electronegativity of O_2 as compared to S_2 that stabilizes the π_p^* orbitals and makes the depopulation of these orbitals during bond formation more difficult. The double bond character of the O_2 molecule is clearly, however, kept in X_2O_2 for the more electronegative X substituents. On the other

dx.doi.org/10.1021/ic3023503 | Inorg. Chem. 2013, 52, 2458−2465

Table 3. Geometrical Parameters of XSeSeX, X_2SeSe, XTeTeX, and X_2TeTe Isomers (Bond Lengths in Å and Angles in deg), Voronoi Charges of X and Y Atoms (in Electrons), and Isomerization Relative Energies (in kJ mol^{-1})[a]

X	r_{Y-Y}	r_{X-Y}	∠YYX	∠XYYX	Q(X)	$Q(Y_1)$	$Q(Y_2)$	r_{Y-Y}	r_{X-Y}	∠YYX	∠XYYX	Q(X)	ΔE_{rel}
				X_2SeSe							XSeSeX		
F	2.161	1.805	106.9	96.9	−0.162	−0.108	0.432	2.200	1.810	107.0	88.9	−0.173	−3.8
Cl	2.180	2.292	109.1	106.0	−0.152	−0.074	0.379	2.240	2.240	108.7	88.6	−0.140	−39.3
Br	2.186	2.469	109.7	108.6	−0.133	−0.068	0.334	2.244	2.402	109.4	88.5	−0.114	−41.8
I	2.198	2.706	110.7	111.5	−0.096	−0.071	0.264	2.266	2.605	109.9	87.7	−0.069	−49.8
H	2.276	1.516	106.5	91.9	0.062	−0.346	0.221	2.356	1.486	96.6	90.4	0.013	−105.9
Li	2.491	2.369	58.2	113.8	0.289	−0.289	−0.289	2.491	2.369	58.2	113.8	0.289	
Na	2.519	2.709	62.2	126.4	0.441	−0.441	−0.441	2.519	2.709	62.2	126.4	0.441	
				X_2TeTe							XTeTeX		
F	2.558	1.935	105.1	92.5	−0.165	−0.120	0.450	2.599	1.957	104.1	89.1	−0.177	9.6
Cl	2.575	2.426	107.3	100.7	−0.168	−0.100	0.435	2.634	2.404	106.1	88.8	−0.168	−25.9
Br	2.580	2.605	107.8	103.4	−0.151	−0.090	0.393	2.640	2.567	106.8	88.7	−0.146	−30.5
I	2.591	2.850	108.8	106.6	−0.119	−0.087	0.325	2.659	2.782	107.5	88.3	−0.104	−39.3
H	2.651	1.712	105.7	90.2	0.034	−0.318	0.251	2.737	1.684	96.1	90.3	−0.010	−85.4
Li	2.881	2.609	56.4	107.9	0.246	−0.246	−0.246	2.881	2.609	56.4	107.9	0.246	
Na	2.909	2.943	60.3	117.5	0.401	−0.401	−0.401	2.909	2.943	60.3	117.5	0.401	

[a]Calculated r_{Se-Se} for Se_2 is 2.198 Å and r_{Te-Te} for Te_2 is 2.597 Å.

hand, for the more electropositive X groups, the charge transfer from the SOMO of $X^\bullet$ to the π_p^* orbitals is favored by the stabilization of these π_p^* orbitals in O_2. This effect is clearly seen in the long O−O bond present in both HOOH and H_2OO species, not far from the bond distance in LiOOLi and NaOONa that corresponds to a single O−O bond. As found for the X_2S_2 isomers, the O−X bond in X_2OO is longer than that in XOOX, now even for the case of X = F. The ∠OOX angle opens up for larger X in both XOOX and X_2OO species. The ∠XOOX dihedral angle in the XOOX isomer is close to 90° in all cases and somewhat decreases for larger X. This dihedral angle becomes close to 180° for X = Li and Na. In these two cases, we get again a unique conformation, but now with a rhombic planar shape.

With respect to the relative energies given in Table 1, in all cases, the isomer XOOX is more stable than X_2OO, and the energy difference increases with the decrease in the electronegativity of X from F (−50.2 kJ mol^{-1}) to H (−196.2 kJ mol^{-1}). The energy differences in the X_2O_2 isomers are in absolute value larger than those corresponding to the X_2S_2 isomers. The smaller electronegativity difference between F and O makes the contribution of double ionic resonance structure **b** less decisive for the relative energy of the FOOF and F_2OO isomers. It must be mentioned that Misra and Marshall analyzed four isomers of I_2O_2, and they found that O_2II (but not the I_2OO species here) and IOIO are isomers more stable than IOOI.[62]

The higher electronegativity of the $O_2^{\bullet\bullet}$ group, which is translated into lower π_p^* orbitals, reduces the transfer of charge from the $O_2^{\bullet\bullet}$ fragment to $2X^\bullet$ for X = halogen when compared to the analogous X_2S_2 species. On the other hand, the charge transfer from X to $O_2^{\bullet\bullet}$ found for X = H, Li, and Na is always larger in X_2O_2.

Table S4 in the Supporting Information contains the results of the energy decomposition analysis carried out for these isomers. The results do not differ significantly from the analysis given in Table 2 for X_2S_2 isomers, except in the following two aspects: first, the large deformation energy of HOOH and H_2OO isomers that is due to the long O−O bond length found in these systems, as discussed above, and second, the fact that the attractive ΔV_{elstat} and ΔE_{oi} terms are in absolute value larger for FOOF than F_2OO. This translates into a more stable FOOF than F_2OO, at variance to what is observed for the FSSF species. As said before, for X more electronegative than Y, the larger the electronegativity difference, the more stable the X_2YY system is. In FOOF, the electronegativity difference is not enough to make F_2OO more stable than FOOF.

If we would like to find X_2Y_2 species with the X_2YY isomer more stable than the XYYX form, we should try less electronegative chalcogen atoms. According to both Pauling[63] and Allen[64] electronegativity scales, $\chi(S) \geq \chi(Se) > \chi(Te)$. For this reason, we analyze in this last section the X_2Se_2 and X_2Te_2 isomers. The results obtained for the geometry, Voronoi charges, and relative energies are given in Table 3. As can be seen, trends in Y−Y and X−Y bond distances are the same as those found for X_2S_2 and X_2O_2. Thus, with no exception, Y−Y distances are longer in XYYX systems and Y−X bond lengths are shorter in XYYX species, FYYF being the only exception to the Y−X bond distance. However, for Y = Se and Te, the F−Y bonds lengths in FYYF and F_2YY species differ by only a few hundredths or even a few thousandths of an Ångström. It is worth noting that experimental results for FSeSeF (d[Se−Se] = 2.25 Å, d[Se−F] = 1.77 Å),[38] F_2SeSe (d[Se−Se] = 2.15 Å, d[Se−F] = 1.77 Å),[38] and BrSeSeBr (d[Se−Se] = 2.241(1) Å, d[Se−Br] = 2.366(1)−2.369(1) Å, ∠SeSeBr = 103.86(5)−104.51(5)°, and ∠BrSeSeBr = 93.58°)[39] are not far from the optimized BP86/QZ4P geometries. On the other hand, the slightly longer Se−Se bond in BrSeSeBr as compared to ClSeSeCl agrees with the reduction in the Se−Se frequency when going from ClSeSeCl to BrSeSeBr.[58] As for the disulfide systems, the XYYX (X = Li and Na; Y = Se and Te) species have a rhombic tetrahedron shape.

Relative energies between the C_2 and C_s isomers for X_2S_2 and X_2Se_2 for each X differ by less than 4 kJ mol^{-1}. This is not completely unexpected since the two atoms have almost the same electronegativity. However, in this case, the FSeSeF isomer is marginally more stable than the F_2SeSe form. On the other hand, and because of the lower electronegativity, X_2Te_2 presents the lowest energy differences between forms XTeTeX and X_2TeTe. Interestingly, F_2TeTe is found about 9 kJ mol^{-1} more stable than FTeTeF. We can conclude that, for X_2Y_2 (Y = O, S, Se, and Te), the XYYX isomer is more stable than X_2YY

dx.doi.org/10.1021/ic3023503 | Inorg. Chem. 2013, 52, 2458−2465

except for difluorides of S, Se, and Te, for which the X_2YY system can coexist with the XYYX isomer. Since the electronegativies of Te and Po are quite similar,[63,64] we expect similar trends for X_2Po_2 as those observed for X_2Te_2.

In this work, we have analyzed the X_2Y_2 (Y = O, S, Se, and Te) species for a series of monatomic substituents X of different electronegativities. For polyatomic X substituents of the type CH_3 or CF_3, the analysis becomes more complex because of other aspects apart from electronegativity (for instance, hyperconjugation), play a determinant role. Here, we report in Table S7 (Supporting Information) the energetic and geometric results for Y = O, S and X = CH_3, CF_3. The molecular structure of these species was experimentally characterized by microwave and electron diffraction studies.[65−68] The results obtained show that trends in the Y−Y bond distances for CH_3 and CF_3 are the same as those found in monoatomic substituents, i.e., the Y−Y bond length is shorter for the more electronegative X = CF_3 substituent (see Table S7, Supporting Information). From a geometric point of view, X = CH_3 yields results quite close to X = H, as expected from the fact that both substituents have similar electronegativities. However, the X = CF_3 results are in between those of X = H and X = I, when they should be closer to X = Cl from electronegativity arguments.[69] It is likely that flow of charge from the π orbital to the σ^*_{C-F} orbital through hyperconjugation is responsible for the lengthening of the Y−Y bond observed in X = CF_3 as compared to X = Cl.

CONCLUSIONS

In this work, we have analyzed the structure and stability of the isomers XYYX and X_2YY (Y = O, S, Se, and Te, and X = H, F, Cl, Br, I, Li, and Na) at the ZORA-BP86/QZ4P level of theory, in the framework of quantitative MO theory in combination with an energy decomposition analysis. We have observed that the X−Y bond weakens as the electronegativity difference decreases, for example, along X = F, Cl, Br, and I. This is in line with the more general phenomenon that increased polarity across bonds leads to enhanced stability.

Furthermore, the XYYX isomers appear to be, in general, more stable than X_2YY because of the short, destabilizing X−X contact in the latter. In the case of X = F, the difference in energy between the isomers is small, but it increases along X = F, Cl, Br, and I due to increasing steric hindrance in X_2YY as X becomes more bulky. For X = Li and Na, only one X_2Y_2 equilibrium structure is obtained in which the alkali atoms adopt a bridging position between the Y atoms of the YY fragment.

Finally, our results show that the character (single versus double) and length of the Y−Y bond can be tuned quite generally by the X−Y electronegativity difference. If X is more electronegative (or electropositive) with respect to Y, the π^* orbital of the YY becomes effectively depopulated (or populated) in X_2YY and in XYYX. This corresponds to a formal decrease (or increase) of the Y−Y bond order and translates into a shortening (or lengthening) of this bond.

ASSOCIATED CONTENT

Supporting Information

Table S1 with the optimized Cartesian coordinates of all studied species. Tables S2 and S3 with experimental and calculated geometrical parameters of XYYX and X_2YY (Y = O and S). Table S4 with the energy decomposition analysis for XOOX and X_2OO species. Table S5 with the geometrical parameters of XTeTeX and X_2TeTe isomers calculated with relativistic and dispersion corrections. Table S6 with calculated Y−Y stretching frequencies. Table S7 with calculated geometrical and energetic parameters of XYYX and X_2YY (Y = O, S and X = CH_3, CF_3). Table S8 with XYYX to X_2YY (Y = O, S) isomerization energies at different levels of theory. Figure S1 with a Pauling electronegativity versus S−S bond length plot for the XSSX and X_2SS series of compounds. This material is available free of charge via the Internet at http://pubs.acs.org.

AUTHOR INFORMATION

Corresponding Author

*E-mail: jordi.poater@udg.edu (J.P.), f.m.bickelhaupt@vu.nl (F.M.B.), miquel.sola@udg.edu (M.S.). Fax: +34-972418356 (M.S.).

Notes

The authors declare no competing financial interest.

ACKNOWLEDGMENTS

We thank the following organizations for financial support: the HPC-Europa program of the European Union, The Netherlands Organization for Scientific Research (NWO), the Ministerio de Ciencia e Innovación (MICINN, project numbers CTQ2011-23156/BQU and CTQ2011-25086/BQU, Ramón y Cajal contract to J.P., and FPI fellowship to M.E.-H.), the Catalan Departament d'Innovació, Universitats i Empresa (DIUE, project no. 2009SGR637 and Xarxa de Referència en Química Teòrica i Computacional), the FEDER fund (European Fund for Regional Development) for the grant UNGI08-4E-003, and the National Research School Combination - Catalysis (NRSC-C). Support for the research of M.S. was received through the ICREA Academia 2009 prize for excellence in research funded by the DIUE of the Generalitat de Catalunya. Excellent service by the Stichting Academisch Rekencentrum Amsterdam (SARA), the Centre de Serveis Científics i Acadèmics de Catalunya (CESCA), and the Barcelona Supercomputing Center − Centro Nacional de Supercomputación (BSC-CNS) is gratefully acknowledged.

REFERENCES

(1) Patai, S., Ed. *The Chemistry of Functional Groups Peroxides*; John Wiley & Sons Ltd.: New York, 1983.
(2) Rappoport, Z., Ed. *The Chemistry of Peroxides*; John Wiley & Sons Ltd.: Chichester, U.K., 2006; Vol. 2.
(3) Kutney, G. W.; Turnbull, K. *Chem. Rev.* **1982**, *82*, 333.
(4) Creighton, T. E. *Proteins: Structures and Molecular Properties*; W. H. Freeman: New York, 1993.
(5) Kochi, J. K. *Free Radicals*; John Wiley & Sons: New York, 1973; Vol. 2.
(6) Benson, S. W.; Shaw, R. In *Organic Peroxides*; Swern, D., Ed.; Wiley Interscience: New York, 1970; Vol. 1.
(7) Cremer, D. In *The Chemistry of Functional Groups Peroxides*; Patai, S., Ed.; John Wiley & Sons Ltd.: New York, 1983; p 1.
(8) Onorato, J. M.; Thorpe, S. R.; Baynes, J. W. *Ann. N. Y. Acad. Sci.* **1998**, *20*, 277.
(9) Baker, A.; Payne, C. M.; Briehl, M. M.; Powis, G. *Cancer Res.* **1997**, *57*, 5162.
(10) Bickelhaupt, F. M.; Solà, M.; von Ragué Schleyer, P. *J. Comput. Chem.* **1995**, *16*, 465.
(11) Jursic, B. S. *J. Comput. Chem.* **1996**, *17*, 835.
(12) Ornellas, F. R. *Chem. Phys. Lett.* **2007**, *448*, 24.
(13) Dobado, J. A.; Martínez-García, H.; Molina; Sundberg, M. R. *J. Am. Chem. Soc.* **1999**, *121*, 3156.
(14) Kaur, D.; Sharma, P.; Bharatam, P. V. *J. Mol. Struct. (THEOCHEM)* **2007**, *810*, 31.

(15) Prascher, B. P.; Wilson, A. K. *J. Mol. Struct. (THEOCHEM)* **2007**, *814*, 1.
(16) Zeng, Y.; Meng, L.; Li, X.; Zheng, S. *J. Phys. Chem. A* **2007**, *111*, 9093.
(17) Jackson, R. H. *J. Chem. Soc.* **1962**, 4585.
(18) Burdett, J. K.; Lawrence, N. J.; Turner, J. J. *Inorg. Chem.* **1984**, *23*, 2419.
(19) Lee, T. J.; Rice, J. E.; Scuseria, G. E.; Schaefer, H. F., III *Theor. Chim. Acta* **1989**, *75*, 81.
(20) Kraka, E.; He, Y.; Cremer, D. *J. Phys. Chem. A* **2001**, *105*, 3269.
(21) Jursic, B. S. *J. Mol. Struct. (THEOCHEM)* **1999**, *459*, 23.
(22) Kuczkowski, R. L. *J. Am. Chem. Soc.* **1963**, *85*, 3047.
(23) Kuczkowski, R. L. *J. Am. Chem. Soc.* **1964**, *86*, 3617.
(24) Kuczkowski, R. L.; Wilson, E. B. *J. Am. Chem. Soc.* **1963**, *85*, 2028.
(25) Minkwitz, R.; Lekies, R.; Lennhoff, D.; Sawatzki, J.; Kadel, J.; Oberhammer, H. *Inorg. Chem.* **1990**, *29*, 2587.
(26) Davis, R. W.; Firth, S. *J. Mol. Spectrosc.* **1991**, *145*, 225.
(27) Shaik, S.; Danovich, D.; Silvi, B.; Lauvergnat, D. L.; Hiberty, P. C. *Chem.—Eur. J.* **2005**, *11*, 6358.
(28) Tonmunphean, S.; Parasuk, V.; Karpfen, A. *J. Phys. Chem. A* **2001**, *106*, 438.
(29) Seel, F.; Budenz, R. *Chem. Ber.* **1965**, *98*, 251.
(30) Gombler, W.; Schaebs, J.; Willner, H. *Inorg. Chem.* **1990**, *29*, 2697.
(31) Brown, R. D.; Burden, F. R.; Pez, G. P. *Chem. Commun. (London)* **1965**, 277b.
(32) Lösking, O.; Willner, H.; Baumgärtel, H.; Jochim, H. W.; Rühl, E. *Z. Anorg. Allg. Chem.* **1985**, *530*, 169.
(33) Cao, X.; Qian, X.; Qiao, C.; Dianxu, W. *Chem. Phys. Lett.* **1999**, *299*, 322.
(34) Mestres, J.; Forés, M.; Solà, M. *J. Mol. Struct. (ThEOCHEM)* **1998**, *455*, 123.
(35) Steudel, R.; Jensen, D.; Plinke, B. *Z. Naturforsch.* **1987**, *426*, 163.
(36) Beagley, B.; Eckersley, G.; Brown, D.; Tomlinson, D. *Trans. Faraday Soc.* **1969**, *65*, 2300.
(37) Marsden, C. J.; Brown, R. D.; Godfrey, P. D. *J. Chem. Soc., Chem. Commun.* **1979**, 399.
(38) Haas, A.; Willner, H. *Z. Anorg. Allg. Chem.* **1979**, *454*, 17.
(39) Katryniok, D.; Kniep, R. *Angew. Chem., Int. Ed. Engl.* **1980**, *19*, 645.
(40) Yokoyama, S. (Sharp Corp., Japan). Manufacture of Dielectric Thin Film Device. Japanese Kokai Tokkyo Koho JP-11354505, 1999.
(41) Bickelhaupt, F. M.; Baerends, E. J. In *Reviews in Computational Chemistry*; Lipkowitz, K. B., Boyd, D. B., Eds.; Wiley-VCH: New York, 2000; Vol. *15*, p 1.
(42) Becke, A. D. *J. Chem. Phys.* **1986**, *84*, 4524.
(43) Becke, A. D. *Phys. Rev. A* **1988**, *38*, 3098.
(44) Perdew, J. P. *Phys. Rev. B* **1986**, *33*, 8822.
(45) Baerends, E. J.; Ziegler, T.; Autschbach, J.; Bashford, D.; Bérces, A.; Bickelhaupt, F. M.; Bo, C.; Boerrigter, P. M.; Cavallo, L.; Chong, D. P.; Deng, L.; Dickson, R. M.; Ellis, D. E.; van Faassen, M.; Fan, L.; Fischer, T. H.; Fonseca Guerra, C.; Ghysels, A.; Giammona, A.; van Gisbergen, S. J. A.; Götz, A. W.; Groeneveld, J. A.; Gritsenko, O. V.; Grüning, M.; Gusarov, S.; Harris, F. E.; van den Hoek, P.; Jacob, C. R.; Jacobsen, H.; Jensen, L.; Kaminski, J. W.; van Kessel, G.; Kootstra, F.; Kovalenko, A.; Krykunov, M. V.; van Lenthe, E.; McCormack, D. A.; Michalak, A.; Mitoraj, M.; Neugebauer, J.; Nicu, V. P.; Noodleman, L.; Osinga, V. P.; Patchkovskii, S.; Philipsen, P. H. T.; Post, D.; Pye, C. C.; Ravenek, W.; Rodríguez, J. I.; Ros, P.; Schipper, P. R. T.; Schreckenbach, G.; Seldenthuis, J. S.; Seth, M.; Snijders, J. G.; Solà, M.; Swart, M.; Swerhone, D.; te Velde, G.; Vernooijs, P.; Versluis, L.; Visscher, L.; Visser, O.; Wang, F.; Wesolowski, T. A.; van Wezenbeek, E. M.; Wiesenekker, G.; Wolff, S. K.; Woo, T. K.; Yakovlev, A. L. *ADF2010.01*; SCM: Amsterdam, 2010.
(46) Te Velde, G.; Bickelhaupt, F. M.; Baerends, E. J.; Fonseca Guerra, C.; van Gisbergen, S. J. A.; Snijders, J. G.; Ziegler, T. *J. Comput. Chem.* **2001**, *22*, 931.
(47) Mezey, P. G.; Hass, E.-C. *J. Chem. Phys.* **1982**, *77*, 870.
(48) Mitchell, D. J.; Wolfe, S.; Schlegel, H. B. *Can. J. Chem.* **1981**, *59*, 3280.
(49) Solà, M.; Gonzalez, C.; Tonachini, G.; Schlegel, H. B. *Theor. Chim. Acta* **1990**, *77*, 281.
(50) Baerends, E. J.; Ellis, D. E.; Ros, P. *Chem. Phys.* **1973**, *2*, 41.
(51) van Lenthe, E.; Snijders, J. G.; Baerends, E. J. *J. Chem. Phys.* **1996**, *105*, 6505.
(52) (a) Grimme, S. *J. Comput. Chem.* **2006**, *27*, 1787. (b) Grimme, S.; Antony, J.; Ehrlich, S.; Krieg, H. *J. Chem. Phys.* **2010**, *132*, 154104.
(53) Morokuma, K. *J. Chem. Phys.* **1971**, *55*, 1236.
(54) Morokuma, K. *Acc. Chem. Res.* **1977**, *10*, 294.
(55) Kitaura, K.; Morokuma, K. *Int. J. Quantum Chem.* **1976**, *10*, 325.
(56) Ziegler, T.; Rauk, A. *Theor. Chim. Acta* **1977**, *46*, 1.
(57) Ziegler, T.; Rauk, A. *Inorg. Chem.* **1979**, *18*, 1558.
(58) Hendra, P. J.; Park, P. J. D. *J. Chem. Soc. A* **1968**, 908.
(59) Bickelhaupt, F. M.; Hermann, H. L.; Boche, G. *Angew. Chem., Int. Ed.* **2006**, *45*, 823.
(60) Deng, L.; Branchadell, V.; Ziegler, T. *J. Am. Chem. Soc.* **1994**, *116*, 10645.
(61) Bickelhaupt, F. M.; Ziegler, T.; von Ragué Schleyer, P. *Organometallics* **1996**, *15*, 1477.
(62) Misra, A.; Marshall, P. *J. Phys. Chem. A* **1998**, *102*, 9056.
(63) Pauling, L. *J. Am. Chem. Soc.* **1932**, *54*, 3570.
(64) Allen, L. C. *J. Am. Chem. Soc.* **1989**, *111*, 9003.
(65) Gase, W.; Boggs, J. E. *J. Mol. Struct.* **1984**, *116*, 207.
(66) Stevenson, D. P.; Beach, J. Y. *J. Am. Chem. Soc.* **1938**, *60*, 2872.
(67) Meyer, M. *J. Mol. Struct.* **1992**, *273*, 99.
(68) Marsden, C. J.; Beagley, B. *J. Chem. Soc., Faraday Trans. II* **1981**, *77*, 2213.
(69) Marriott, S.; Reynolds, W. F.; Taft, R. W.; Topsom, R. D. *J. Org. Chem.* **1984**, *49*, 959.